

Preliminary Simulation Study of Doppler Reflectometry

Yuta ISHII, Hitoshi HOJO, Atsushi MASE¹⁾, Masashi YOSHIKAWA, Makoto ICHIMURA, Yusuke HARAGUCHI and Tsuyoshi IMAI

Plasma Research Center, University of Tsukuba, Tsukuba 305-8577, Japan

¹⁾*Art, Science and Technology Center for Cooperative Research, Kyushu University, Kasuga 816-8580, Japan*

(Received 10 December 2009 / Accepted 11 May 2010)

A preliminary simulation study of Doppler reflectometry is performed. The simulations solve Maxwell's equations by a finite difference time domain (FDTD) code method in two dimensions. A moving corrugated metal target is used as a plasma cutoff layer to study the basic features of Doppler reflectometry. We examined the effects of the full width at half maximum (FWHM) of the electromagnetic waves and the corrugation depth of the metal target. Furthermore, the effect of a nonuniform plasma is studied using this FDTD analysis. The Doppler shift and velocity are compared with those obtained from FDTD analysis of a uniform plasma.

© 2010 The Japan Society of Plasma Science and Nuclear Fusion Research

Keywords: Doppler reflectometry, diagnostic simulation, FDTD code, plasma flow velocity

DOI: 10.1585/pfr.5.S2094

1. Introduction

Doppler reflectometry is considered to be a promising diagnostic for measuring the poloidal plasma flow and radial electrostatic field in magnetically confined plasmas. When an electromagnetic wave is injected into the plasma with a finite tilt angle, it is reflected and scattered under the Bragg condition at the cutoff density layer. By detecting the Doppler frequency shift in the reflected wave signals, we can measure the plasma's poloidal flow velocity and thus obtain the radial electrostatic field, which is the origin of the $\mathbf{E} \times \mathbf{B}$ drift. However, the interpretation of the reflected signals is difficult and typically must be validated by other diagnostic results or with the help of a theoretical model. At low turbulence, we can apply Born approximation to the analysis [1]. However when the turbulence level is too high to neglect multiple scattering, this approximation is incorrect. If we can assume a large enough distance from the receiver position to the cutoff layer $x_c \gg 2\pi c/\omega$ and a large turbulence radial correlation length $l_{cx} \gg 2\pi c/\omega$, the WKB approximation can be applied [2]. However when the electromagnetic wave is transmitted at only a few wavelengths, this approximation is incorrect.

In this paper, the finite difference time domain (FDTD) method is applied to turbulence analysis. This method can be applied to multiple scattering simulations. Electromagnetic waves are injected to a moving corrugated metal target. The reflected waves are analyzed by Fourier analysis to measure the Doppler shift. The relationship between the velocity of the metal target and the Doppler shift of the reflected waves is studied by varying the full width at half maximum (FWHM) of the incident beam width and

the depth of the corrugation. Then the relationship between the Doppler shift of the electromagnetic waves and the change in plasma flow velocity is identified.

2. Analytical Method

The analysis domain is the two-dimensional space (x, z) . The waves propagate in the radial direction with tilt angle θ to the x -axis. The reflected waves satisfy the Bragg resonance condition. The electromagnetic component (E_y, B_x, B_z) is considered.

Maxwell's equations are used to describe the electromagnetic field.

$$\nabla \times \mathbf{E} = -\frac{\partial \mathbf{B}}{\partial t}, \quad (1)$$

$$\frac{1}{\mu_0} \nabla \times \mathbf{B} = \mathbf{J} + \frac{\partial \mathbf{E}}{\partial t}. \quad (2)$$

Here \mathbf{E} , \mathbf{B} , and \mathbf{J} represent the wave electric field, magnetic field, and current density, respectively. \mathbf{E} and \mathbf{J} satisfy the equation of motion

$$\frac{\partial \mathbf{J}}{\partial t} = -\varepsilon_0 \omega_{pe}^2 \mathbf{E}, \quad (3)$$

where ε_0 and ω_{pe} are the permittivity of vacuum and the plasma frequency, respectively. The difference in the x components of Eq. (1) is shown as follows [3].

$$B_x \left(\mathbf{x}, z + \frac{\Delta z}{2}, t + \frac{\Delta t}{2} \right) = B_x \left(\mathbf{x}, z + \frac{\Delta z}{2}, t - \frac{\Delta t}{2} \right) + \frac{\Delta t}{\Delta z} \{ E_y(\mathbf{x}, z + \Delta z, t) - E_y(\mathbf{x}, z, t) \}. \quad (4)$$

Other components and expressions are obtained by the same method. The spatial configuration of the electromagnetic field is shown in Fig. 1.

author's e-mail: ishii_yuta@prc.tsukuba.ac.jp

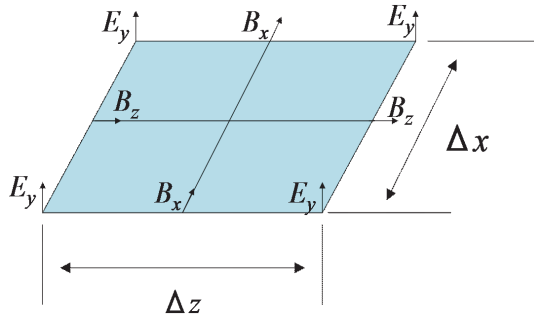


Fig. 1 Electromagnetic field elements used in this analysis. Computational domain is divided in this cell.

The Mur boundary condition is used as the absorbing boundary condition [3]. This applies to the four corner edges of the computation domain in the wave equation. The boundary condition of electromagnetic radiation propagation in the direction of positive x is given by,

$$\frac{1}{c} \frac{\partial}{\partial t} \left(\frac{1}{c} \frac{\partial}{\partial t} + \frac{\partial}{\partial x} \right) E_y - \frac{1}{2} \frac{\partial^2}{\partial z^2} E_y = 0. \quad (5)$$

3. Simulation Model

We obliquely launch the electromagnetic waves in the two-dimensional (x, z) analytic space. The simulation parameters are as follows, the tilt angle θ , pulse duration and frequency are 15° , $1/3$ ns, and 36.23 GHz, respectively. We chose a pulse duration of $1/3$ ns because analysis is difficult if interference occurs between the incident and reflected waves during measurement of the electric field. The reflected (scattered) signal at the metal surface satisfies the Bragg condition. We apply fast Fourier transform (FFT) analysis to the reflected signal at the incident point. The Bragg condition is given by,

$$mk_{\perp} = 2k_0 \sin \theta_{\text{tilt}}, \quad (6)$$

where k_0 and m are the incident wavenumber and diffraction order, respectively. The model for the metal target and electromagnetic wave propagation is shown in Fig. 2. The electromagnetic wave starts at $(x, z) = (0, 100)$ and propagates direction at a tilt angle of θ of 15° . The green lines show the equipotential lines of the propagating electric field. The color bar shows the amplitude of the electric field. The lines inside the metal are electromagnetic waves leaking into the metal.

The metal target is set in the domain according to the following expression.

$$x \geq 100 + A \sin(k_{\perp} z - \omega t). \quad (7)$$

The depth of the metal corrugation can be varied by changing the value of A . The function of the incident wave is divided into a time dependent component and a space dependent component on the z axis and is given by

$$f(z) = \sin(k_{\perp} z) \exp[-((z - 100)/\sigma)^2], \quad (8)$$

$$f(t) = \sin(\omega t). \quad (9)$$

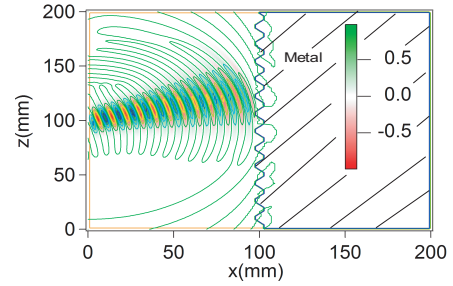


Fig. 2 Analytic metal model in two dimensional space and electric field patterns.

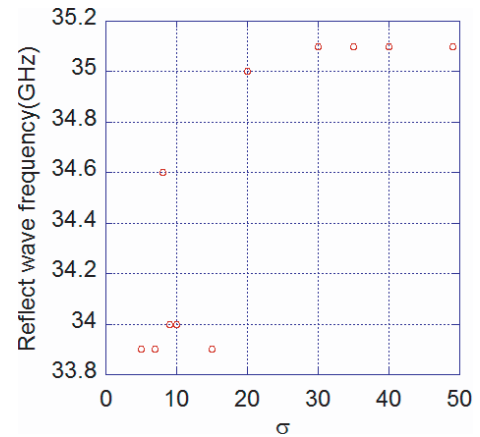


Fig. 3 Numerical results of the Doppler peak frequency as a function of the FWHM of the incident beam.

The FWHM of the incident beam width is varied by changing the value of σ .

3.1 Doppler shift as a function of the FWHM of the incident beam

The frequency of the reflected wave is analyzed by an FFT for various values of the FWHM of the incident beam width. The frequency versus the FWHM is shown in Fig. 3. The amplitude A is 2.5 mm, the toroidal turbulence wavenumber k_{\perp} is 415.2 m^{-1} , and the speed of the metal was assumed to be 2% of the speed of light. The wavenumber k_{\perp} has an error of 2.7 m^{-1} .

The amplitude has a large effect on the reflective surface of the metal when the FWHM of the beam is small. Thus it is unsuitable for measuring the flow velocity. The reflected wave contains the effects of both flow velocity and the partial shape of the reflection surface. When the FWHM (σ) is larger than 30, the Doppler peak frequency reaches a the constant value.

3.2 Doppler shift as a function of corrugation depth of the metal target

The speed of the metal was assumed to be 4% of the speed of light. The FWHM is assumed to be $\sigma = 48.3$. The toroidal turbulence wavenumber k_{\perp} is 415.2817 m^{-1} .

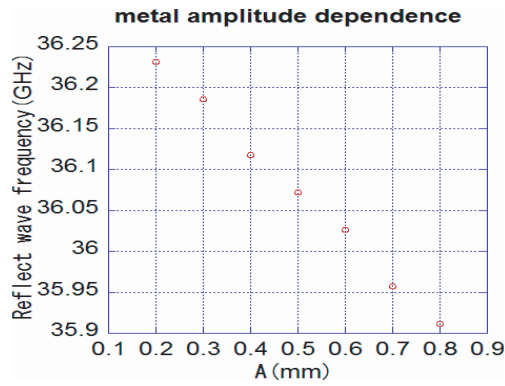


Fig. 4 Numerical results of the Doppler peak frequency as a function of corrugation depth of the metal target.

The numerical results of the Doppler peak frequency as a function of the corrugation depth of the metal target are shown in Fig. 4. It is difficult to analyze the case of small corrugation depth, since we would have to make a large number of meshes. The frequency of the reflected wave decreases with the amplitude A .

4. Plasma Model

The density distribution shown in Fig. 5 is assumed. The plasma density distribution obeys the following equation which includes a term representing the turbulence obeys by the term representing the turbulent term $\delta n_e(r, t)$ and it takes the value of no effect for a certain time of turbulence $n_{e0}(r)$.

$$n_e(r, t) = n_{e0}(r) + \delta n_e(r, t). \tag{10}$$

The RMS plasma density turbulence is 2%, and it is expressed as

$$\delta n_e(x, z, t) = A \sin(k_z z + k_x x + \omega t). \tag{11}$$

Here, the wavenumber in the z direction k_z satisfies the Bragg condition. We assumed $\sigma = 48.3$ the tilt angle $\theta = 15^\circ$ and the frequency is 38.3 GHz. Electromagnetic radiation propagates in the plasma according to the Bragg condition.

Figure 6 shows the time evolution of the electric field at $x = 10$ mm.

In Fig. 6, the waves around $z = 50$ and $t = 0$ is the incident wave. The large amplitude of the reflected wave around $z = 250$ and $t = 2000$ satisfies the Bragg condition of $m = 0$, and the amplitude of the reflected wave around $z = 50$ and $t = 2000$ (circled region shown in Fig. 6) satisfies the Bragg condition of $m = -1$.

We examined the correlation between the plasma flow and the Doppler shift. The result of the calculation is shown in Fig. 7. The Doppler shift of the electromagnetic wave is linearly related to the plasma flow with an offset caused by the shape of the reflecting surface. However, there is also an offset between the estimated Doppler shift

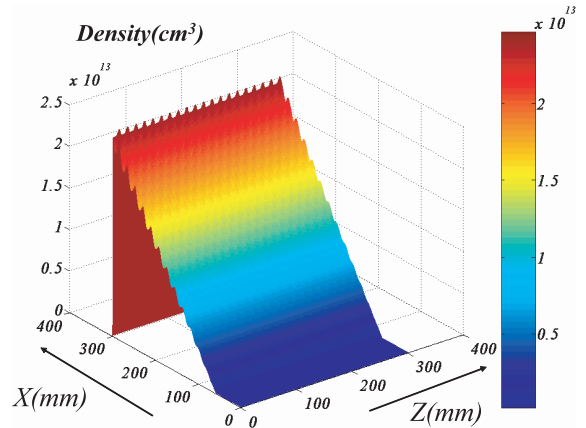


Fig. 5 Plasma density profile used in this analysis.

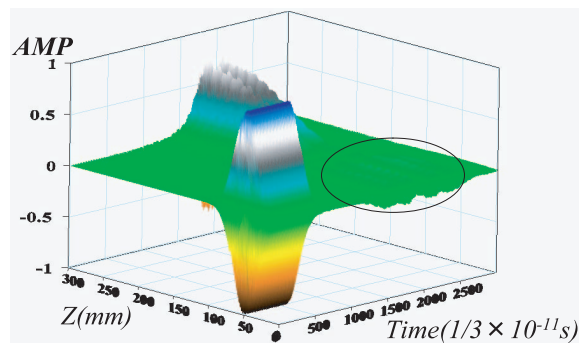


Fig. 6 Time evolution of the electric field at $x = 10$ mm indicating Bragg resonance in the plasma shown in Fig. 5.

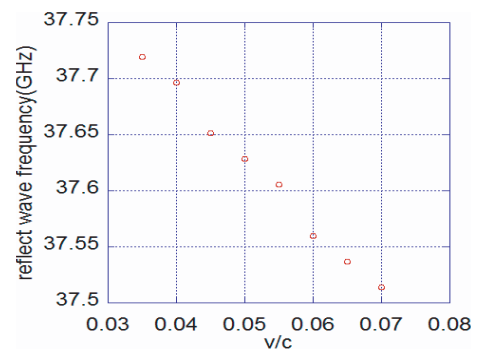


Fig. 7 Relationship between the Doppler shift of the reflected wave and the plasma flow velocity.

and the simulation result. This offset decreases with increasing input pulse length. Thus its efficient is negligible if we use a longer input pulse length. However, we can study the relationship between the Doppler shift of the electromagnetic wave and the change in plasma flow velocity at this pulse length.

5. Summary

In this study, Doppler reflectometry is simulated. We examine the dependence of the Doppler shift on the

FWHM of the incoming electromagnetic wave and on the corrugation depth of a metal target. We also examine the relationship between the plasma flow and the Doppler shift. The Doppler shift is different at the same speed when the FWHM of the electromagnetic wave is small. As a result, we found that the relationship between the target velocity and the Doppler shift is not as straightforward as expected. When σ reaches a constant value, the Doppler shift settles at a certain constant value. The Doppler shift is proportional to the corrugation depth of the metal surface. Thus, we clearly observed a correlation between the Doppler shift of the reflected waves and the flow velocity of the plasma.

In the future, we plan to include an analytical solution in the FDTD analysis to advance the calculation, including condensation with a mirror and three-dimensional analysis, and to compare the results with two-dimensional analyses.

Acknowledgement

The authors wish to thank the member of the A. Mase

group and of the Plasma Research Center, University of Tsukuba for helpful discussions. This work was partly supported by Grants-in-Aid for Scientific Research from the Ministry of Education, Science, Sports and Culture, Japan (Nos. 16082205, 30116660, and 20360186)

- [1] F. da Silva, S. Heurax and M. Manso, *Nucl. Fusion* **46**, S816 (2006).
- [2] E. Z. Gusakov, A. V. Surkov and A. Yu Popov, *Plasma Phys. Control. Fusion* **47**, 959 (2005).
- [3] Uno Tsuru, "Finite Difference Time Domain Method for Electromagnetic Field and Antennas" CORONA PUBLISHING CO., LHD.
- [4] M. Ignatenko, A. Mase, L. G. Bruskin, Y. Kogi and H. Hojo, *Rev. Sci. Instrum.* **75**, 3810 (2004).
- [5] J. Schirmer, G. D. Conway, E. Holzhauer, W. Suttrop, H. Zohm and the ASDEX Upgrade Team, *Plasma Phys. Control. Fusion* **49**, 1019 (2007).
- [6] M. Hirsch, E. Holzhauer, J. Baldzuhn, B. Kurzan and B. Scott, *Plasma Phys. Control. Fusion* **43**, 1641 (2001).